Journal of Achievements in Materials and Manufacturing Engineering
VOLUME 43
ISSUE 1
November
2010

FEM applications to the analysis of passive solar wall elements

K. Lenik*, D. Wójcicka-Migasiuk
Department of Fundamental Technology, Lublin University of Technology,
ul. Nadbystrzycka 38, 20-618 Lublin, Poland
* Corresponding author: E-mail address: wz.kpt@pollub.pl

Received 12.09.2010; published in revised form 01.11.2010

Analysis and modelling

ABSTRACT

Purpose: The evaluation of heat propagation effectiveness through passive solar modules of different construction in relation to selected process conditions by means of computer simulation.
Design/methodology/approach: The analysis of heat transfer through laminar structures in transient states by means of FEM and its verification on small scale models during laboratory tests.
Findings: The paper presents the application of FEM and its methodology of computations for the established conditions on both sides of laminar structures specific for solar passive-thermal modules. The results are compared to small scale experimental results. The verification of the analysis leads from particular conclusions concerning the procedure of simulations towards general comments on the application of real modules.
Research limitations/implications: The research has been carried out by means of software suitable for field analysis with some limitations to 3D which have been specified but their influence on usefulness of results is only minor. The verification on a small scale model is necessary and reliable in terms of the research consistence.
Practical implications: Finite Element Method exploited in the applied methodology of investigation can be successfully used as a tool to examine energy transfer at considerations on different laminar structures. The subject of the research, i.e. solar passive modules confirmed their usefulness for energy demand reduction but with some identified restrictions.
Originality/value: The use of small scale solar modules to verify FEM analysis and the combination of both analyses to determine the applicability of modules in real conditions of solar energy conversion in different building objects.
Keywords: Numerical techniques; Engineering design; Materials and engineering databases; Education and research trends

Reference to this paper should be given in the following way:
K. Lenik, D. Wójcicka-Migasiuk , FEM applications to the analysis of passive solar wall elements, Journal of Achievements in Materials and Manufacturing Engineering 43/1 (2010) 333-340.

1. Introduction

One of the basic problems in different aspects of passive buildings is the reduction of energy demand for space heating. The paper describes that this issue can be partially solved thanks to the improvements in laminar structures known as Trombe-Mitchell's walls [1][3] that has been identified in the result of the carried analysis. Heat propagation through laminar structure can be graphically expressed in the way it is presented in Fig. 1. Particular symbols mean: r – radiation, *sz*- transparent zone, s-solar, A_b-absorption, t-temperature, I - radiation intensity, α - convection, p - plane, *pow* - air, ε - emission.

There are typical elements that can be considered within the overall construction of solar walls, i.e.: massive elements, air gap and a transparent zone such as glass or transparent insulation

(TIM element). They have been presented in Fig. 1. Together with the direction of solar energy propagation and its conversion. However the complex ideas of energy transfer through laminar structures used in buildings have been known for scientists, there is no common appreciation to the usefulness of solar passive applications at higher latitudes and cold climate of winter conditions. The described research is going to fill this gap and to give some scientific explanation, experimentally verified to solve at least one of the passive house problems in severe climates.

The analysis have been performed in two directions: firstly - FEM analysis by means of Flux CEDRAT® [4] on a real scale structure model and secondly – computations of a small scale model with the use of the theory of similarity. Moreover the tests have been carried out on a small scale model in a laboratory chamber. All results show the usefulness of the analyzed object for the purpose of energy demand reduction for building heating and the effectiveness of FEM for the purpose of the analysis [5][8]. The paper describes the procedures and the results that enable the author to formulate such advantageous conclusions.

Trombe walls provide effective energy transport into the building interior preventing simultaneously from heat loss at night time. This is possible thanks to the special construction that can be considered as thermal diode. Transparent insulation elements gather visual radiation and become thermal insulation in the opposite direction of heat transfer, thanks to low thermal permeability of organic glass material of which the capillary system is made. If, additionally, this construction is well ventilated, excessive heat transport into the building is forced. This can be realized by flap elements located in channels on the top and the bottom of the wall (indicated in Fig.3). The orifice area should not exceed 2% of wall surface and must block opposite draught. The best materials for Trombe's massive wall constructions are: rubble concrete, common brick, crushed stone aggregate, stone and even water in leakproof containers. Thickness d_b of an average massive element in solar walls ranges between 40 cm for concrete and 35 cm for bricks. The external surface should be covered with possibly black velvet film of selective properties to reduce reflection. Its absorptive properties are characterized by A_{bpow} . Some special attention should be paid to remove all thermal bridges from such elements. Moreover, there is another element of different character i.e.: transparent insulation d_{sz} . This construction, suitable for our climate, consists usually of two parallel glass panels filled with aerogel or another material of capillary structure such as honeycomb perpendicular to the wall. Usually the distance between the panels is about 12 cm and they are made of silicon glass, organic glass or polycarbonates, polyethylene, or any plastic recommended by manufacturers of special proved properties adapted for this application. In Mediterranean regions, only one glass panel is sufficient for winter season but then additional shades are necessary for summer months. This undesired heat transfer can also be reduced by movable curtains, shutters either equipped with insulation material or not. Shading cornices are also suitable in some cases but they matter in the field analysis rather as the shape of the field but do not change material properties.

The other element is an air gap providing the additional heat flow between the wall and a room if necessary in either of directions. This is adjusted by means of flaps open at the top of the wall if warm air is to get inside and closed if the air is not warm enough or too hot.

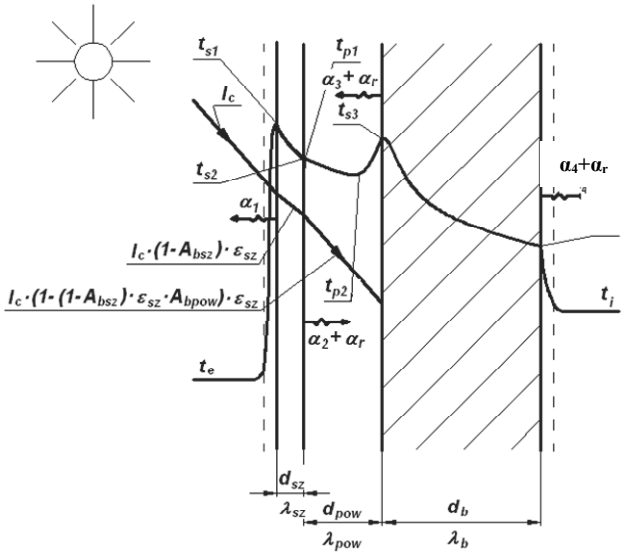

Fig. 1. Typical structure of solar walls ($\Sigma d \cong 0.8$m)

2. Results and discussion

The laboratory stand to test solar walls was designed as an insulated chamber consisted of two compartments. One of them simulated ambient conditions (left side of the laminar structure presented in Fig.1) and the other one simulated room conditions (right side). The artificial sun generated radiation intensity at the following levels: 250 W/m^2, 350 W/m^2 and 600 W/m^2 considered as a prevailing range for the central eastern region of Poland for intermediary season such as early spring or late autumn. The actual value was measured by means of a pyranometer (Kipp&Sonnen CM3). There was a limited possibility to simulate temperature conditions and it ranged between 15 and 25 ^{o}C (temperature sensors). Only temperature measurements were taken inside the compartment that substituted room climate but it is sufficient for the purpose of heat transfer. Test series duration was usually 24 hrs in one sequence.

In the case of simulation by means of FEM, the test conditions can be established as required. This made possible to divide the conditions into the ranges specific for particular year period.

The heat flows through solar walls by means of radiation, conduction and natural convection in transient conditions. The decisive factor that has the influence on that flow is radiation. The other ways of the exchange depend on construction parameters and the total thermal balance of buildings. The factor diversifying the heat transfer is the construction. When massive element is made of lime-sand bricks then the main role of such solar wall to collect gains from radiation and to transport them through convection with the air flow. If this massive element is of high thermal capacity (e.g. rubble concrete) then the heat accumulation is decisive and convection has dual character: convection in a closed gap within a few degree range or in a vertical open gap, depending on flap settings. The assumption then is that both sides of the gap are of equal temperature.

Table 1.
Specific conditions established for simulated periods

Sub-range of simulated period	Specific conditions	
	Solar radiation W/m^2	Ambient Temperature range ^{o}C
Winter - night	0	- 10
Winter - day	250	- 5
Early spring night	0	0
Early spring day	350	10
Spring day	600	15
Summer day	850	20
Autumn day	450	15
Late autumn night	0	0
Late autumn day	350	10

The two dimensional temperature field that can be plotted in each point of a wall cross section can show isothermal lines connecting points of the same temperature (T-dT, T, T+dT). They do not cross at the end of the investigated field area (domain) but discontinue. Temperature changes in the directions crossing isothermal lines and the maximal difference per length unit, so called temperature gradient, occurs in the direction normal to these lines. The temperature gradient is a vector value directed along this normal towards the isothermal line. The idea of temperature field is presented by means of a hypothetic three-dimensional (dx, dy, dz) element in Fig. 2, which can serve as the example of a massive element in a ventilated solar wall. The most general approach assumes that this element is moving and contains internal heat sources dQ_v.

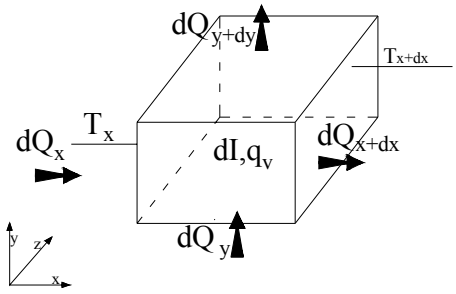

Fig. 2. Energy balance for elementary volume dV (Z flux assumed normal)

The energy balance, presented in Fig.2 on elementary volume dV, is performed for assumed time range dt and determines elementary increase of its total enthalpy dI (eq.1).

$$(dQ_x - dQ_{x+dx}) + (dQ_y - dQ_{y+dy}) + (dQ_z - dQ_{z+dz}) + dQ_v = dI \quad (1)$$

Theoretical equation of heat transfer for transient conditions that is used by Flux 2D assumes that solar walls contain static isotropic elements and is formulated as eq. 2.

$$C\frac{dT}{d\tau} + div(-\lambda(gradT)) = q_v \quad (2)$$

At stationary conditions, it has the form as eq. 3.

$$div(-\lambda(gradT)) = q_v \quad (3)$$

The equation solver is in this case adapted for three-dimensional fields. It establishes in two-dimensional field xy the identity along the third z-axis of an investigated element up to the length of 1 m, which makes possible to solve spatial problems. Assuming that thermal bridges do not exist, internal heat sources do not occur in solar walls.

The explicitness of solutions to heat transfer differential equations require:

- geometric conditions that determine the shape and dimensions of the heat exchange surface of the investigated body,
- physical conditions that determine physical properties of material and thermal - physical properties of flowing medium,
- boundary conditions,
- time distribution of source capacity,
- turbulence model suitable for the particular case of investigated phenomenon.

At radiation, boundary conditions are determined by Stefan – Boltzmann's Law for grey surfaces. The explicitness conditions determine the only one solution to the particular problem that is continuously dependent on boundary conditions.

The boundary conditions and the initial condition enable to determine temperature field in all elements at any time. The initial condition specifies the temperature distribution in the investigated field region at t=0. The boundary conditions are divided in four kinds.

I. The boundary condition of the first kind (Dirichlet's) determines the temperature distribution T_s on external surfaces in time:

$$T_s(\tau) = f_I(\tau) \quad (4)$$

II. The boundary condition of the second kind (Neumann's) is given by the distribution of heat flux density q_s on external surfaces in time:

$$q_s(\tau) = f_{II}(\tau) \quad (5)$$

III. The boundary conditions of the third kind (Fourier's) determine the temperature T_p of the medium flowing round the surface and the combined coefficient α of thermal convection and radiation dependent on turbulence models in all points of the domain boundary composed of the material of the conduction coefficient and in time:

$$\lambda_s\left(\frac{\delta T}{\delta n}\right)_s = \alpha(T_p - T_s) \quad (6)$$

where: $\alpha = \alpha_c + \alpha_r$

The radiation coefficient α_r (between boundary surfaces on both sides of a gap s_1, s_2) is expressed as eq. 7:

$$\alpha_r = \frac{C}{T_{s1} - T_{s2}}\left[\left(\frac{T_{s1}}{100}\right)^4 - \left(\frac{T_{s2}}{100}\right)^4\right] \quad (7)$$

where: C - grey body radiation coefficient.

IV. The boundary conditions of the fourth kind (contact) become important when thermal conduction on both sides of the contact surface is determined by Fourier's Law. In this case the conditions include the equation of temperature ($T_{s1} = T_{s2}$) and the equation of thermal flux density:

$$q_s = -\lambda_1\left(\frac{\delta T_1}{\delta n}\right) = -\lambda_2\left(\frac{\delta T_2}{\delta n}\right) \tag{8}$$

When any of surfaces is rough then the contact has additional thermal contact resistance (r_s). The cavities are filled with a fluid of any kind but of lower thermal conductivity than the materials in the investigated contact. The temperature difference occurs in this contact: $T_{s1}-T_{s2} = r_s q_s$. and this boundary condition has the form of eq. 9:

$$q_s = -\lambda_1\left(\frac{\delta T_1}{\delta n}\right)_{s1} = -\lambda_2\left(\frac{\delta T_2}{\delta n}\right)_{s2} = h_s(T_{s1} - T_{s2}) \tag{9}$$

where: $r_s = h_s^{-1}$

If there is convection on the material surface then the condition of the third kind is suitable. When α is high ($\cong 10^3$) the condition becomes the first kind. If radiation is dominant or the surface is adiabatic the second condition is suitable (also in the case when chemical reactions or phase changes occur on surfaces). Generally, when Neumann boundary conditions are established the description of the transient state is:

$$C\ \frac{\delta T}{\delta \tau} + \lambda\ \frac{\delta T}{\delta n} = -q - \alpha(T_s - T_a) - \varepsilon C_c\left[\left(\frac{T_{s1}}{100}\right)^4 - \left(\frac{T_{s2}}{100}\right)^4\right] \tag{10}$$

where:
T – temperature, K,
q – heat flux density, W/m^{2}K,
τ - time, s,
α - convective heat transfer coefficient, W/m^{2}K,
ε - surface emissivity,
λ - thermal specific conductivity, W/mK,
C – grey body constant, W/m^{2}K^4.

Instantaneous values can be computed thanks to the transient analysis performed for the theoretical equation describing transient heat transfer that makes the basis for computational algorithms in Flux 2D and have the form expressed by eq. 2, assuming isotropic character of particular wall layer compound materials.

The derivative could take into account also velocity changes in particular directions if the field is moving, but this is not the case of a wall. Solving problems in two-dimensional *xy* field by means of Flux2D, one can assume the equality of construction along invisible z-axis to 1 m (as typical dimension of solar wall modules), according to eq. 11:

$$c_p\rho\left(\frac{\delta T}{d\tau}\right) = \lambda\left(\frac{\delta^2 T}{\delta x^2} + \frac{\delta^2 T}{\delta y^2} + \frac{\delta^2 T}{\delta z^2}\right) + q_v \tag{11}$$

The accepted attempt makes possible to solve the problem on the model area that is presented in Fig.1 with the addition of two rooms within one floor building. Moreover, Neumann's boundary condition has been applied to surfaces assumed as the building envelope.

It is assumed that temperature in rooms is to be maintained at the level of 20 °C, thus means that heating is necessary. The simulation had to check if the resulting temperature does not drop below 20 or raises above 25 °C. Otherwise, the solution would not be of any use for residential or public buildings, but still could be useful for the purpose of storage (goods).

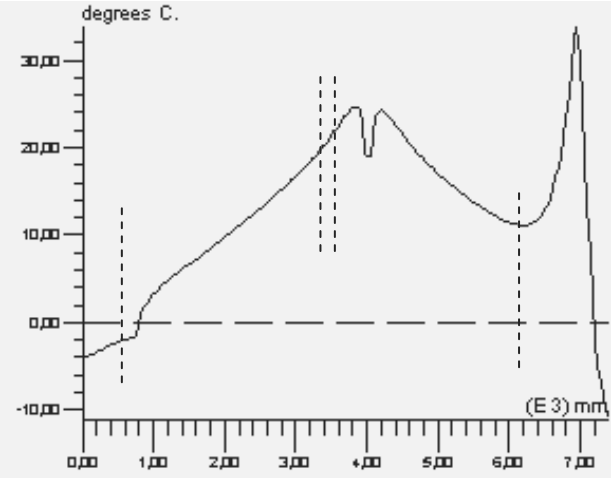

Fig. 3. Instantaneous temperature graphs (winter-day)

The majority of calculations have been performed for a ground floor two-room building model. The huge number of results obtained from measurements and simulations has to be grouped in relation to particular consideration. First assumption is: thermal losses through a solar wall element do not exceed a relevant standard wall element (of u<0.3 W/m^{2}K). Then the computation is not just a simple calculation of u value, because of the air gap providing air flow to the room, and must result from the complex research. FEM analysis provides a very convenient comparable value such as temperature at domain boundaries – layer surface temperature in the form of instantaneous graphs (Fig. 3). Dashed lines indicate room wall surfaces. The resulting room temperature is the mean of the indicated in Fig.3. This particular graph is taken from transient state computations at 0.2 m after 24-hour simulation. The results collected in the form of this graph need the following explanation:

1. The example shows distinct diversity of isotherms in both rooms.
2. The period of simulation is obviously too short for such large thermal capacity as in the case of a massive wall.
3. The graph indicates the disadvantageous thermal conditions in the outlets of bottom air channels.

The selection of mean temperature values for particular layer surfaces and levels are presented in Table 2.

It is very important in the analysis to indicate if resulting temperature on particular wall surface makes possible to maintain thermal comfort conditions (at least within ±2 °C range about 20 °C) through the whole year subsequent seasons. The considerations include also the integrated conventional heating (wall radiators). The aspects and details of this integration were presented by the author in the reference [1], [11].

Table 2.
Mean temperature values for particular layer surfaces and heights above the floor

Layer surface – domain depth (l)	Temperature above the floor level (m)	(°C)
Glass external surface, left – l=0m	0.2	-4
	0.8	-4
	1.6	-3.9
Glass panel external surface of capillary structure, right l=0.1 m	0.2	-3.6
	0.8	-2
	1.6	0
Brick wall channel surface l=0.3m	0.2	-3
	0.8	3
	1.6	10
Massive element at room side surface l=0.8 m	0.2	-1
	0.8	10
	1.6	10
Int. wall element, left surface l=3.8m	0.2	24
	0.8	36
	1.6	34
Int. wall element, northern room side surface l=4.2m	0.2	20
	0.8	34
	1.6	22
Northern external wall, room side surface l=7m	0.2	26
	0.8	14
	1.6	0
Northern external l=7.5m	0.2	-10
	0.8	-10
	1.6	-10

The results collected in Table 2 need the following explanation from thermal point of view:
1.Observed temperature difference between 0.2 and 1.6 m ensures the thermal comfort overall in both rooms but indicates regions of droughts coming from lower part of a solar wall.
2.Droughts between wall surfaces and heater can be omitted.
3.The solar wall elements are protected from very humid conditions resulting e.g. from heavy rains by means of TIM elements. Thus, no additional changes of thermal conductance is to be considered because of water content.

The comparison between temperature distribution in the northern wall with standard insulation and in the southern wall with a solar module shows that they are usually located in different temperature ranges and the southern one can generate heat by itself.

Simulation procedure used for the analysis consists of the following modules [4]:

Preflu 2D module serves for geometry. The geometrical model is created by the user and then Finite Element Mesh is plotted for the model. The more complex is the element of the whole geometry, the more mesh nodes should be created. This means that the mesh density is not equal in the whole geometrical model of the building

CSLMat module enables the introduction of material properties. Heat transfer coefficients are treated as material properties assigned to particular surfaces, respectively as the analysis requires.

Physical models are created in PROPHY module. This is also the procedure to introduce boundary conditions for the model and the inputs. The boundary conditions have been established as mentioned in Chapter 3.1. and the inputs have been restricted to the following limits: maximal temperature allowed to the heat source (modeled in the glass panel) is 80°C, thermal power is constant on the whole source and does not exceed 800 W/m2, ambient temperature can vary between – 15°C and 25°C, power for radiators established separately as indicated below in the chapter with results.

Solver 2D module generates isotherm maps either for steady state or for transients but in separated procedures.

PostPro module enables further analysis of results, i.e.: time animations, graphical presentation of temperature waveforms and heat flux waveforms, if applicable. The heat flux in this analysis has been treated as constant for hourly mean values.

The approach to FEM analysis needs the following assumptions [6],[7][9][10]:
1. Mesh density does not have to be equal in the whole structure as the real cross-section area is 21 m^2 . It is not homogeneous and it contains comparatively small elements such as metal shuttles, corner shapes of air outlets and reinforce, where thermal flux propagates in the different way in comparison to the massive wall structure or air volume in rooms.

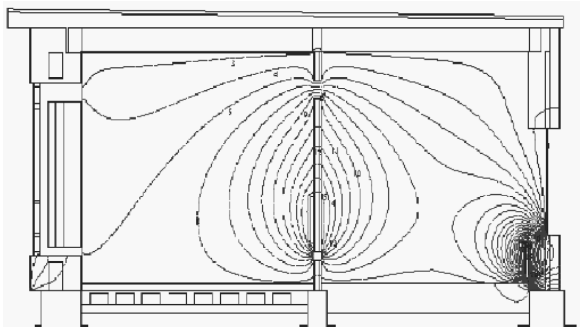

Fig. 4. Temperature distribution in the whole domain

Thus, the mesh is to be dense in small elements and rare in big ones. This makes the total number of nodes less than 600 and computations - optimal.
2. The accuracy of computations does not depend on the quantity of nodes if they are generated as described above.

The final results obtained for simulation sessions have the form presented in Fig. 4, which gives some point of view on the information one can get from the analysis. The real image in Flux is much more informative because temperature values are provided and colors reflect the gradient. This image, however, does not reflect the plasticity of the final picture because the scale is too small for such spacious cross-section, small elements are invisible and there is no color, thus isotherm values are not visible. The additional information for this particular layout is - it has been obtained for cold winter.

Moreover, this system of two rooms, the ambience and the solar wall has been constructed as a physical model consisted of two chambers connected with a wall model. It is very important

that test experiments provided the confirmation for FEM analysis, although, the procedure of measurements delivers the information rather on heat flux density than on isotherms. Moreover, the Tables 1 and 2 suggest some assumptions that can be taken up to analyze building envelope throughout the whole year changes of conditions.

Fig. 5. The verification of modeling on two climatic chambers combined through a solar wall model in the laboratory [11]

Laboratory tests have been carried out to verify simulation methods and its results. The main purpose to carry out temperature measurements was the determination of temperature distribution on subsequent surfaces of solar passive elements. Such elements are tested either in laboratory conditions or in practice of used buildings. But it follows from the research carried mainly by Fraunhoffer Institute, Germany and also by other European research centers that tests on buildings in use are burden with deviations caused by the diversity of usage. It is usually better to perform such tests on a simple laboratory model and then adapt the results to particular purpose and practice [12], [13], [14].

The verification of simulations have been performed on a small scale model (0.8 m^2) by means of measurements taken at subsequent layer surfaces. Fig. 5 presents the image of a test stand composed of two chambers connected through a solar wall and the data acquisition system employing software Genie®. The front chamber serves for the purpose of the ambience and the rear one plays the role of a room. The sun is artificial (40, 60, 80 W) and this makes possible to simulate spring and summer day/night conditions.

Fig. 6 presents the cross section of the model wall which is in compliance to what has been presented in Fig. 1. Model dimensions have been established mainly to fit the chambers and thus the relevance to real objects is not equally proportional in all elements. The materials used to construct the model are: concrete of density about 2000 kg/m^3, made of keramsite aggregate; window glass panel and steel construction.

The air circulation between two chambers is maintained by means of horizontal tubes, which are located at the top and at the bottom of this wall element and play the role of ventilation in a real object. The concrete surface has been painted with black matt enamel on the side of glass and with white enamel on the side of the chamber.

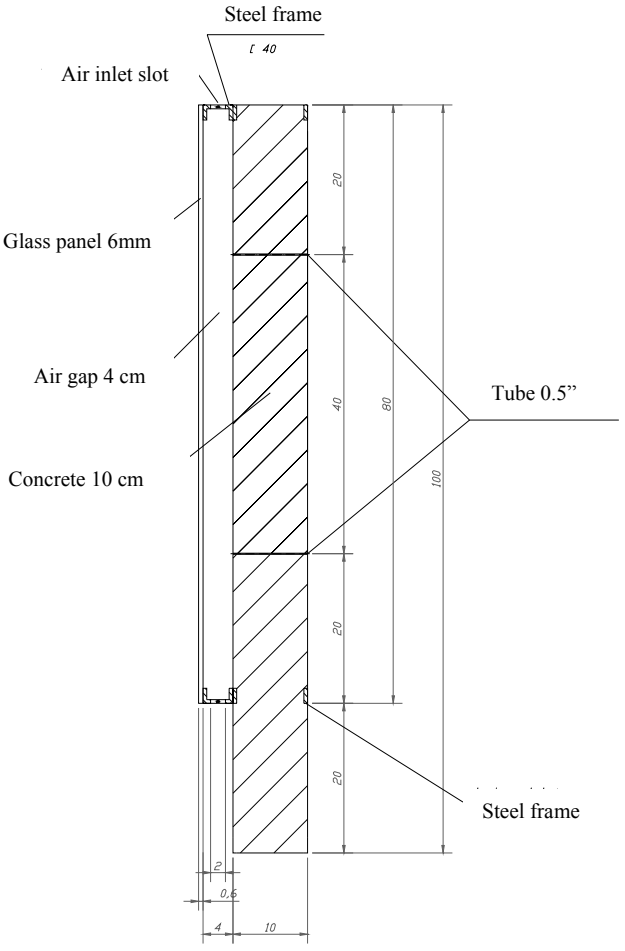

Fig. 6. Cross section of a solar wall model, for which the measurements have been taken.

The results of temperature measurements on subsequent surfaces are presented in the form of graph in Fig.7, with the relevance to the symbols indicated in Fig. 1. The values are presented for day summer conditions. The additional remark refers to solar temperature t_{s1}, which is a hypothetic value of ambient air temperature on shadowed surface when transferred heat is equal to the one at the ambient temperature t_e with simultaneous transfer of solar radiation heat. This makes that solar temperature is always higher that the ambient one, except for night, of course. This is expressed by eq.12:

$$t_{sl} = t_e + \frac{A_b \cdot I_c}{\alpha_e} \qquad 12$$

where:
t_e- ambient temperature (solar day), *ºC*
A_b- surface absorbtion coefficient,
I_c- total solar radiation intensity (insolation), W/m^2
α_e- heat transfer coefficient at external wall surface, W/m^2K.

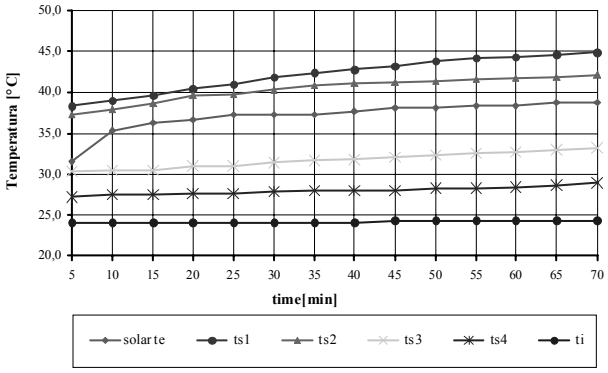

Fig. 7. Measurements on the model

The other collection of thermal analysis results is presented in Fig. 8., where the temperature changes are shown as a continuous waveform in time. The image is far from sinusoidal shape because this is not only ambient conditions (temperature and insolation) that determine the temperature inside the building but there is also the influence of conventional heating and the heating – cooling time constant of the solar wall. The steady state has not been reached in the presented period. The visible temperature drop shows the time lag caused by the thermal inertia of the wall massive element. This graph shows the results computed on the solar wall surface in the room interior. Some other computations and tests were performed for water wall construction. There is no distinctive difference between the two types o solar walls, so there is no need to diversify results. The water wall type was successfully installed in America [13] where it served also for the purpose of utilization of plastic containers but in European localization there is no need to introduce such novelty of anyhow less reliable construction than concrete elements.

Fig. 9 presents the dynamics of temperature at the level of feet i.e. 0.25 m over the floor after 5 days of good radiation. This image shows that one can more likely observe draughts in the bottom of the room than on the level of a head (in comparison to Fig. 8) because of diversity of temperature. This can be easily avoided in real objects if instead of traditional wall radiators, floor low temperature heating systems are used.

The comparison between simulation and tests on a small scale model let us formulate the conclusion that the simulations give even more useful results than tests. It is mainly because of that scale. Time constants at heating of massive elements, within established range of temperature, are about 6 hours.

The total room has it at least three times longer (depending on volume and construction). The comparatively big real object have long time constants of about several days. That is why they are usually used in transient states caused by varying input conditions, in practice. Transient simulation enable us to analyze a number of configurations of input conditions and results. In the contrary, the model shows us the behavior of a structure when steady state has been reached and is useful for total computations of energy demand and losses and they confirm the findings from simulations. Moreover the precision of graphic presentation is nearly not limited for simulation software and the consequence can only be visible in time consumption by computers. The precision of making details in models and then temperature

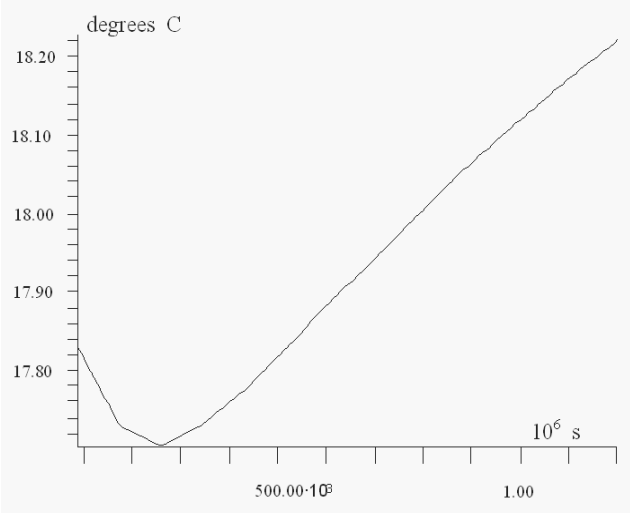

Fig. 8. Temperature waveform as time dependent variable at 1.6 m over the floor in the southern room.

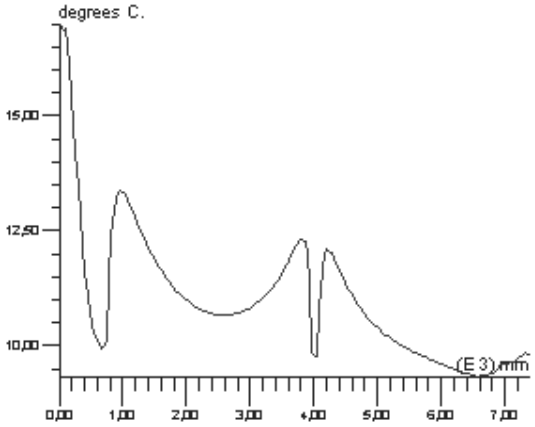

Fig. 9. Temperature instantaneous values at the level of 0.25 m over the floor after 5 days of good radiation.

measurements of particular small parts require high precision temperature sensors of micro dimensions which disadvantageously increases the cost of tests.

3. Conclusions

The presented scope of research refers to two combined problems, i.e.: to the selection and evaluation of materials and to the heat transfer through structures constructed with these materials.

The presented procedures of Finite Element Method have been successfully used at construction elements in the variety of areas for years. This presentation adds some special application to complex structures composed not only of heat conducting solid materials and transparent modules but also of convective nature air spaces and slots together with thermal radiation occurrence

which is crucial if low energy buildings such as passive houses are considered.

What is even more important the ease of this type of analysis can add the value to the planned refurbishments and all purpose modernizations in many municipal sectors in the phase prior to the design instead of time consuming and expensive existing building inventorying *in situ*. This should be particularly taken into account when numerous objects are to be rebuild in the regions where older technology have been applied so far.

Particular conclusions can be derived in relation to the application of such passive structures in mid-European countries. This is visible that typical Trombe – Mitchell's construction cannot be successfully used for the whole year because:

- Insulation even by two glass panels is insufficient for winter.
- Solar radiation in summer often exceeds the needs.

But in the intermediary season of fall (spring/autumn), solar walls prove their usefulness and thus make possible to reduce heating period and energy demand in total thanks to the solar gain in several weeks within the range of the whole heating period.

There is also a very useful solution to the problem of insulation, i.e. transparent panels. Thanks to the capillary structure they let radiation in and prevent from thermal losses because of air trapped within capillary and its material – organic glass - of insulation properties.

Moreover, the shading can be realized by means of insulated folded blinds and with the help of leaf trees.

References

[1] D. Wójcicka–Migasiuk, A. Zając, Thermal analysis of rooms with solar walls, Archives of Civil Engineering PAN LIII 1 (2007) 161-173.

[2] L. Zalewski, S. Lassue, B. Duthoit, M. Butez, Study of solar walls - validating a simulation model, Building and Environment 37/1 (2002) 109-121.

[3] M. Santamouris, E. Dascalaki, Passive retrofitting of office buildings to improve their energy performance and indoor environment: the OFFICE project, Building and Environment 37/6 (2002) 575-578.

[4] Cedrat.Flux2D Tutorial of thermal steady and transient state: V. 7.50., France, 2000.

[5] J. Szargut, Numerical modeling of temperature fields, WNT, Warsaw, 1992 (in Polish).

[6] K. Lenik, M. Paszeczko, Z. Durjagina, K. Dziedzic, M. Barszcz, The surfach self-organization In process friction and corrosion of composite materials, Archives of Materials Science and Engineering 30/1 (2008) 9-12.

[7] F. Ayari, T. Lazghab, E. Bayraktar, Parametric Finite Element Analisis of Square cup deep drawing, Computational Materials Science and Surface Engineering 1/2 (2009) 106-111.

[8] W. Kajzer, A. Kajzer, J. Marcinek, FEM analysis of compression screws used for small bone treatment, Journal of Achievements in Materials and Manufacturing Engineering 33/2 (2009) 189-196.

[9] J. Trzaska, L.A Dobrzański, A. Jagiełło, Computer programme for prediction steel parameters after heat treatment, Journal of Achievements in Materials and Manufacturing Engineering 24/2 (2007) 171-174.

[10] K. Lenik, S. Korga, FEM applications to model friction processes in plastic strain conditions, Archives of Materials Science and Engineering 41/2 (2010) 121-124.

[11] D. Wójcicka-Migasiuk, Heat transfer analysis in solar walls, LTN, Lublin, 2008 (in Polish).

[12] Proceedings of CISBAT 2009 International Conference, EPFL, Lausanne, Switzerland Renewables in a changing climate – from nano to urban scale, 2009.

[13] D. Chwieduk, R. Domański, M. Jaworski, Editors of Renewable Energy Innovative Technologies and New Ideas, Warsaw, 2008.

[14] A. Popko, Integrated information conversion systems, Energy Market 2/63 (2006) 37-41 (in Polish).